Ksenzenko, M., Konstantinov, A. A., Khomutov, G. B., Tikhonov, A. N. & Ruuge, E. K. (1983) *FEBS Lett.* 155(1): 19–24.
Link, T. A., Haase, U., Brandt, U. & Von Jagow, G. (1993) *J. Bioenerg. Biomembr.* 25(3): 221–232.
Longo, V. D., Gralla, E. B. & Valentine, J. S. (1996) *J. Biol. Chem.* 271(21): 12275–12280.
Longo, V. D., Liou, L. L., Valentine, J. S. & Gralla, E. B. (1999) *Arch. Biochem. Biophys.* 365(1): 131–142.
Muller, F. (2000) *J. Amer. Aging Assoc.* 23: 227–253.
Muller, F., Crofts, A. R. & Kramer, D. M. (2002) *Biochemistry* 41(25): 7866–7874.
Muller, F. L., Roberts, A. G., Bowman, M. K. & Kramer, D. M. (2003) *Biochemistry* 42(21): 6493–6499.
Sharp, R. E., Moser, C. C., Gibney, B. R. & Dutton, P. L. (1999) *J. Bioenerg. Biomembr.* 31(3): 225–233.
Skulachev, V. P. (1996) *Q. Rev. Biophys.* 29(2): 169–202.
von Jagow, G. & Link, T. (1986) *Methods Enzymol.* 126: 253–271.

LOW-TEMPERATURE ABSORBTION AND MAGNETIC CIRCULAR DICHROISM OF THE FOUR HAEMS OF THE CYTOCHROME b_6f COMPLEX

Sindra Peterson Årsköld[1], Jörgen Ström[2], John F. Allen[2], Elmars Krausz[3]. [1]Department of Biochemistry and [2]Department of Plant Biochemistry, Center for Chemistry and Chemical Engineering, Lund University, PO Box 124, S-22100 Lund, Sweden. [3]Research School of Chemistry, Australian National University, Canberra ACT 0200, Australia

Keywords: Cytochrome b_6f, Cytochrome c_i, MCD, absorption, spectroscopy

INTRODUCTION

The cytochrome (cyt) b_6f complex is situated in the thylakoid membrane, where it mediates linear electron transfer between photosystems II and I and performs cyclic electron transfer. Both processes result in proton translocation across the membrane, creating an electrochemical gradient for ATP synthesis. Homologous to the mitochondrial cytochrome bc_1 complex, cyt b_6f incorporates cytochrome f (a c-type cytochrome) and an Fe_2S_2 protein, constituting the linear electron pathway from hydroplastoquinone to plastocyanin, and cytochrome b_6, containing the haem groups b_H and b_L involved in cyclic electron transfer. Unlike the mitochondrial complex, the b_6f complex also contains a chlorophyll (chl) a, a β-carotene (car), and a fourth haem, haem c_i (reviewed by Allen (2004)). The presence of haem c_i at the stromal quinone binding site came as a surprise when the X-ray crystal structure was solved last year, for cyt b_6f purified from the unicellular green alga *Chlamydomonas reinhardtii* (Stroebel et al 2003) and from the thermophilic cyanobacterium *Mastigocladus laminosus* (Kurisu et al 2003). The Fe of haem c_i is penta-coordinate, with water (or hydroxide) the only axial ligand. This indicates a high-spin configuration of the haem, which would explain why it has not been predicted from previous spectroscopic studies.

We used low-temperature, high-precision optical polarization spectroscopies to investigate the chromophores of the cyt b_6f complex. In particular, magnetic circular dichroism (MCD) was used to monitor the four haem groups in reducing and oxidizing environments. As the number of haem groups is unambiguously known from the crystal structure, and MCD shows quantitative signals from cytochromes poised in any redox and spin state, this approach promises further rigorous results.

MATERIALS AND METHODS

Cyt b_6f was isolated from 12-day-old pea leaves, following Hurt and Hauska (1981), with the dialysis step replaced by a Phenyl (High Sub) column, followed by concentration of the fractions of interest using Microsept 10 K Omega.

For the reduced samples, dithionite was added in excess and left to incubate in the dark, on ice, for 5–10 min. Then, glycerol was added to give a final concentration of 60% (v/v), and the mixture was rapidly inserted into a quartz-windowed cell and glassed into He(l). For the oxidized samples, periodate replaced dithionite.

The spectrometer (described by Peterson Årsköld et al (2003)) allows simultaneous detection of absorption and (M)CD, making analysis of (M)CD spectra in terms of the corresponding absorption spectra exact and reliable. The MCD traces presented are the differences between spectra recorded at +5T and −5T.

RESULTS AND DISCUSSION

1.7-K Absorption and MCD Spectra of cyt b_6f. In Fig. 1A, the 1.7-K absorption spectrum of cyt b_6f is displayed, and the origin of each spectral contribution specified. Chl a dominates the spectrum, with a strong Soret band at 420 nm and the Q_y transition at 670 nm. The vibrational side-bands of the Q_y peak and the Q_x transition are present in the 550–650 nm region. These features identify the pigment as a regular chl a. The β-car absorption is also visible, at 488 nm.

The peaks at 548 and 551.5 nm have been assigned to the Q_x and Q_y transitions of the reduced form of cyt f (Schoepp et al 2000). The vibrational side-bands are discernible in the 500–550 nm region. The presence of these features establishes that in our preparation, cyt f is reduced to a significant extent, while the other haem groups are oxidized. The absorption features of oxidized, low-spin haem are spread over 400–600 nm, but are too weak to stand out under the chl a Soret band. However, these features are accompanied by strong MCD signals, clearly visible in Fig. 1B (solid line). Despite its strong aborption, chl does not contribute to the MCD in this region.

Low-spin oxidized haem gives rise to a strong MCD C-term at 420 nm, along with a series of weaker features reaching above 600 nm. C-terms are paramagnetic in origin, and are distinguished by strong temperature dependence. The 50-K MCD (Fig. 1B, dashed line) identifies the cyt C-term from other absorptions. The derivative-shaped MCD A-term associated with reduced, low-spin haem around 550 nm is unaffected by temperature, as is the weak chl B-term at 670 nm. The A-term of reduced cyt f is shown in detail in Fig. 2 (thick, solid lines). The positive and negative components of the A-term establish the exact wavelengths of the Q transitions, and

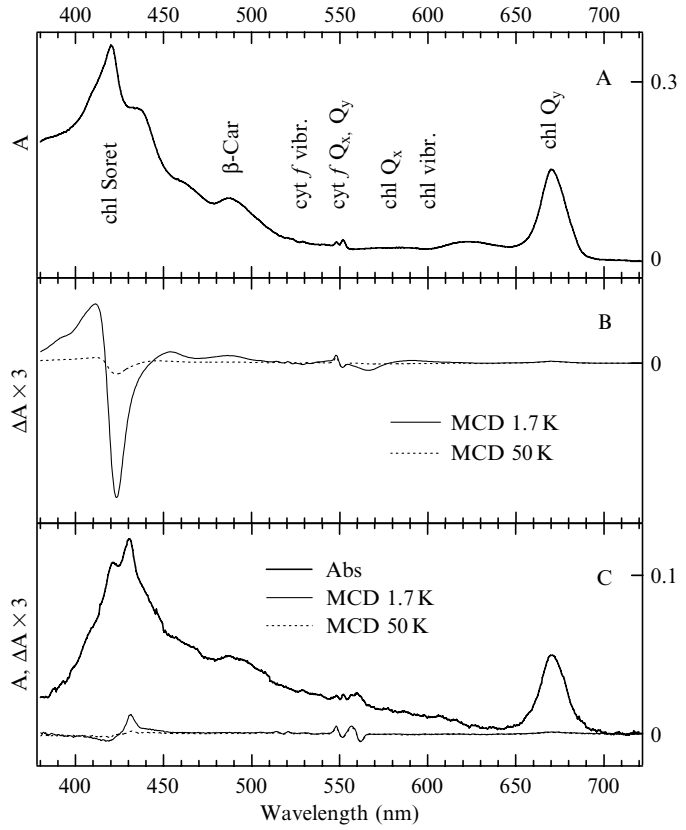

Figure 1: (A) 1.7-K absorption spectrum of the cyt b_6f complex. (B) The corresponding MCD at 1.7 K (solid) and 50 K (dashed). (C) 1.7-K absorption, 1.7-K and 50-K MCD of fully reduced cyt b_6f. The data are plotted to equal chl Q_y intensities in all samples, for quantitative comparison. The MCD data are magnified 3 times compared with the absorption.

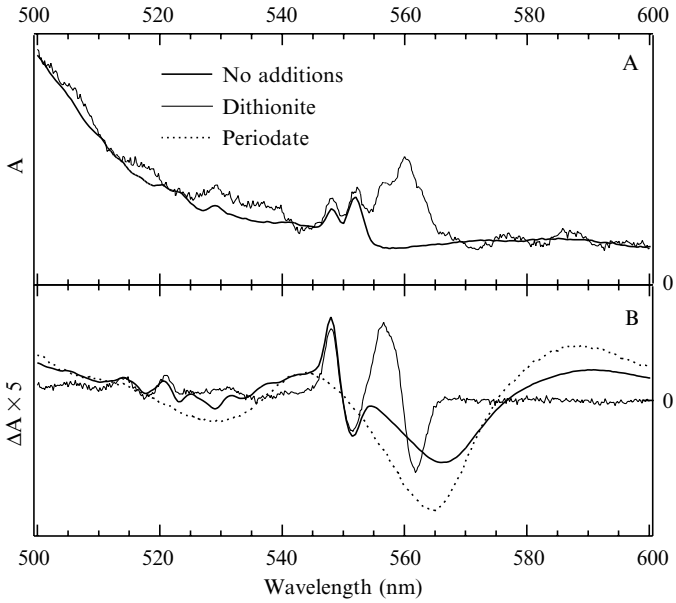

Figure 2: 1.7-K absorption (A) and MCD (B) of cyt b_6f without reactants, with dithionite (all cyt reduced), and with periodate (all cyt oxidized; MCD only). The data are plotted to equal chl Q_y intensities. The MCD data are magnified 5 times.

the vibrational side-bands are clearer in the MCD than in the absorption.

MCD Spectra of Fully Reduced and Fully Oxidized cyt b_6f. *Fully reduced cyt b_6f.* Figure 1C shows the 1.7-K absorption (thick, solid line) and MCD (thin solid and dotted lines) of cyt b_6f reduced by dithionite. Under these conditions, there is no sign of the low-spin, oxidized cyt C-term. At 430 nm however, a temperature-dependent MCD signal characteristic of high-spin, ferric haem has appeared. The thin, solid lines in Fig. 2 show the green spectral region in detail. Features from reduced cyt *f* are similar to those in the untreated samples. Additional peaks are seen at 556.6 and 561.8 nm which can be assigned to a superposition of reduced haems b_H and b_L (Schoepp et al 2000). The MCD A-term accompanying these peaks is broad and asymmetric, supporting the conclusion that this is a composite signal.

Fully oxidized cyt b_6f. The dashed line in Fig. 2B shows the MCD of cyt b_6f under oxidizing conditions. All signs of reduced haem are gone, while a strong C-term from oxidized haem is present. There are no discernible absorption features in this region (not shown).

Quantitative Analysis of the Haem Content of each cyt b_6f Sample. Cytochromes give rise to clearly distinguishable and quantitative MCD signals in the ferrous low-spin, ferrous high-spin, and ferric low-spin states. Ferric high-spin haem also gives rise to a distinctive MCD signature, but this signal is too small to be detected among other haem signals. The various forms of cytochrome MCD have been comprehensively reviewed by Cheesman et al (1991).

In the periodate-treated sample (Fig. 2B, dashed line), 100% of the low-spin population is oxidized, as seen by the absence of A-terms around 550 nm and the presence of a strong C-term in the same region. Using this C-term to quantify the C-term present in the non-treated sample (thick, solid line), we find that 60% of the low-spin population is oxidized in this sample. From the location of the single A-term in the non-treated sample, we conclude that the remaining 40% of low-spin haem is reduced cyt *f*.

In the dithionite-treated sample, there is no oxidized low-spin haem. The cyt *f* A-term at 550 nm was not increased by the treatment, indicating that it was fully reduced in the untreated sample. The magnitude of the cyt *b* absorption compared to cyt *f* indicates that cyt b_H and b_L are fully reduced (Schoepp et al 2000) under these conditions.

In the present report, we demonstrate the presence of high-spin ferrous haem in cyt b_6f under reducing conditions (Fig. 1C). We assign this to cyt c_i. Consistent quantification of the ferric cyt MCD signals requires that ferric cyt c_i is high-spin as well. Comparing the high-spin, reduced cyt MCD signal at 430 nm (Fig. 1C) to the literature (Cheesman et al 1991), it appears about 50% as strong as expected. This low intensity could mean that only half of the cyt c_i population is reduced by dithionite, leaving half in the (not discernible) ferric high-spin state. This would require quite a low redox potential of cyt c_i, which is perhaps less likely, seeing that it is positioned next to the inner quinone binding site and is therefore likely to undergo frequent redox chemistry. Alternatively, the nature of cyt c_i could be such that the ferrous MCD signal is inherently weak. This would be expected if the spin-orbit coupling of the excited states is low (Cheesman et al 1991).

CONCLUSIONS

Our MCD data from the cyt b_6f complex under different conditions are consistent with cyt c_i being in a high-spin configuration and cyt f, b_H and b_L in low-spin configurations, irrespective of redox state.

In the untreated sample, cyt f is fully reduced (low-spin), cyt b_L and cyt b_H are fully oxidized (low-spin), as is cyt c_i (high-spin). Periodate fully oxidizes cyt f, cyt b_H and cyt b_L (low-spin), as well as cyt c_i (high-spin). Dithionite reduces cyt f, cyt b_H and cyt b_L fully (low-spin), and reduces cyt c_i (high-spin) to 50% or more.

We believe cyt c_i to be fully reduced by dithionite, but with inherently weak MCD, indicating weak spin-orbit coupling between the excited states.

ACKNOWLEDGMENTS

SPÅ acknowledges grants from *Kungliga Fysiografiska Sällskapet i Lund* and *Stiftelsen Landshövding Per Westlings Minnesfond*. We thank Derek Bendall for suggestions on sample preparation.

REFERENCES

Allen, J. F. (2004) *Trends in Plant Sci.* 9: 130–137.

Cheesman, M. R., Greenwood, C. & Thomson, A. J. (1991) *Adv. Inorg. Chem.* 36: 201–255.

Hurt, E. & Hauska, G. (1981) *Eur. J. Biochem.* 117: 591–599.

Kurisu, G., Zhang, H., Smith, J. L. & Cramer, W. A. (2003) *Science* 302: 1009–1014.

Peterson Årsköld, S., Masters, V. M., Prince, B. J., Smith, P. J., Pace, R. J. & Krausz, E. (2003) *J. Am. Chem. Soc.* 125: 13063–13074.

Schoepp, B., Chabaud, E., Breyton, C., Verméglio, A. & Popot, J.-L. (2000) *J. Biol. Chem.* 275: 5275–5283.

Stroebel, D., Choqet, Y., Popot, J.-L. & Picot, D. (2003) *Nature* 426: 413–418.

ADDITION OF THE Q_I SITE INHIBITOR ANTIMYCIN CHANGES THE ENVIRONMENT OF THE 2Fe2S CLUSTER AT THE Q_O SITE OF THE CYT bc_1

Jason W. Cooley, Fevzi Daldal. Department of Biology, University of Pennsylvania, Philadelphia, PA 19104-6018

INTRODUCTION

Most of the bacterial ubihydroquinone (UQH_2): cytochrome (cyt) c oxidoreductases (cyt bc_1) contain three subunits (cyt b, cyt c_1 and the FeS protein) carrying four prosthetic groups (b-high, b-low and c_1 hemes and a 2Fe2S cluster, respectively), and form two active sites, Q_o (UQH_2 oxidation) and Q_i (UQ reduction) on the p and n sides of the membrane. A unique aspect of Q_o site catalysis lies in the fact that the FeS subunit initiates a bifurcated oxidation of the UQH_2, with the first electron being conveyed to the 2Fe2S cluster, which ''shuttles'' its electron via a rotational displacement from the cyt b to the cyt c_1, and the other to the b-low heme (Trumpower et al 1978, Crofts et al 1999). The movement can be divided into two portions, a micro- and a macro-movement, reflecting the oscillations of the 2Fe2S at the cyt b surface and its swing to near the cyt c_1, respectively. Whether the Fe-S movement is a simple tethered diffusion, or is tightly regulated to insure correct Q_o site turnover remains unclear. Of note, is that when electron transfer through the b hemes to the UQ at the Q_i site is blocked by the addition of Q_i site inhibitors such as antimycin, the electrons derived from the UQH_2 oxidation at the Q_o site do not leak back into the chain consisting of electron transfer through the 2Fe2S to the c_1 heme (Gray et al 1994, Crofts et al 1999). However, under these conditions, the Fe-S may retain the ability to oxidize UQH_2 at the Q_o site via possible by-pass reactions, but only at extremely low rates (~1–2%) compared to uninhibited turnover (Muller et al 2001).

Currently, how such a strict control is achieved during the multiple turnovers of the Q_o site oxidation reactions is unclear, and many proposals attempt to address this issue. A possibility would be to limit the ability of the 2Fe2S cluster to return to the Q_o site when not appropriate (e.g. in the low potential pathway there is no thermodynamically stable repository for the second electron derived from UQH_2 oxidation). If and how this may be accomplished remains an open question. We present here the first spectral evidence documenting that the events at the Q_i site affect the steady state interactions of the 2Fe2S with the occupant of the Q_o site. These interactions appear to be dependent on: the presence of the antimycin at the Q_i site, the ability of the Fe-S subunit to undergo a micro-movement, and on the Q/QH2 occupancy of the Q_o site of the cyt bc_1.

MATERIALS AND METHODS

Bacterial strains and growth conditions. All *R. capsulatus* strains, their construction and phenotypes are as described previously (Darrouzet et al 2000).

Preparation and spectroscopic analysis of ordered membrane sample. Membrane isolation and ordered sample preparation is described in detail in Cooley et al 2004. Antimycin and HQNO concentrations were approximately 10 and 30 μM per ~30 mg/ml total membrane protein, respectively. Chemical reduction was by addition 5 mM Na-Ascorbate.

RESULTS/DISCUSSION

Competitive Inhibition at the Q_i Site by Antimycin Alters the EPR Spectral Shape of Ordered Membrane Samples. To address the possibility that antimycin causes an alteration of the steady-state position of the 2Fe2S (i.e. less Fe-S at the cyt b Q_o site), ordered membrane samples from wild type (WT) *R. capsulatus* membranesx and a variety of hinge region strains, the +nAla mutants (+1Ala, +2Ala, +3Ala; known to be slowed in the macro-movement, deficient in the macro-movement, or devoid of both the macro- and micro-movements of the Fe-S, respectively (Darrouzet et al 2000, Cooley et al 2004) were treated with antimycin and subjected to oriented EPR analysis. Oriented EPR analysis yields specific information about the relative orientation (and relative numbers of different orientations) of the [2Fe2S] cluster in a given sample, as well as increased spectral resolution of a given transition in the EPR spectrum.